QUDIT ISOTOPY

ARTHUR JAFFE, ZHENGWEI LIU, AND ALEX WOZNIAKOWSKI

Harvard University, Cambridge, MA 02138, USA

February 9, 2016

ABSTRACT. We explore a general framework to understand isotopy in the braiding of qudits and its relation to entanglement. This involves the use of diagrams to represent qudits and to implement some standard quantum information protocols. We introduce qudit Pauli operators X, Y, Z algebraically and also diagrammatically, and use them in our discussion. We explain some alternative models for diagrammatic structures and briefly discuss relationships between them. Our results rely on algebraic and topological relations discovered in the study of planar para algebras. In summary, this work provides bridges between the new theory of planar para algebras and quantum information, especially in questions involving entanglement.

CONTENTS

1. Introduction

The topological approach to quantum computation became important with Kitaev's 1997 posting proposing an anyon computer—a paper that only appeared some five years later in print [16]. In §6 of the arXiv version, he described the braiding and fusing of anyonic excitations in a fault-tolerant way. Freedman, Kitaev, Larsen, and Wang explored braiding further [8], motivated by the pioneering work of Jones, Atiyah, and Witten on knot invariants and topological field theory [14, 2, 19]. Kauffman and Lomonaco remarked that the braid diagram describes maximal entanglement [15].

In this paper we give diagrammatic interpretations of qudits, using the framework of *planar para algebras* introduced in [12]. This picture is compatible with the description of qudit entanglement. We illustrate in Figure 1 the use of a braid to represent the entanglement provided by the conjunction of a Hadamard and CNOT gate. We construct
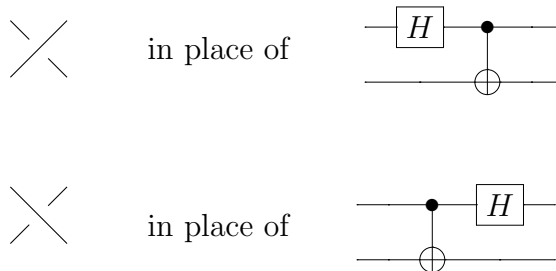

FIGURE 1. Entangling, unitary solution of the Yang-Baxter equation on the left, and entangling quantum circuit on the right.

a similar maximally entangling qudit-braid. We use braids such as in Figure 1, but generalized to include particle excitations illustrated in Figure 2, with the notation explained in §2. We illustrate how to obtain entanglement distribution and entanglement-swapping. One can

employ this braid to obtain a partial topological quantum computer. This is a consequence of the Brylinskis' remarkable criterion.[1]

FIGURE 2. Qudit-braid relation.

We show the *qudit-braid* relation in Figure 2, which illustrates how a particle moves under the braid crossing. There are many different ways to present transformations and qudits in quantum information theory. We compare some of these methods, but in order not to distract from our main discussion, we postpone this to §6. There we give different concrete models to realize qudits and transformations.

In §5.2, we give one example in detail, in which we realize a quantum circuit using the one-string model (that we employ throughout the bulk of the paper). This model illustrates how we take advantage of using *topological isotopy*—a property central to the structure of planar para algebras. In §6.4 we apply our four-string model to construct controlled gates, motivated by the recent paper of Hutter and Loss [10].

2. NOTATION

2.1. **The Parafermion Algebra.** The *parafermion algebra* is a $*$-algebra with unitary generators c_j, which satisfy

$$c_j^d = 1 \quad \text{and} \quad c_j c_k = q\, c_k c_j \quad \text{for} \ \ 1 \leqslant j < k \leqslant m. \tag{1}$$

Here $q \equiv e^{\frac{2\pi i}{d}}$, $i \equiv \sqrt{-1}$, and d is the order of the parafermion. Consequently $c_j^* = c_j^{-1} = c_j^{d-1}$ where $*$ denotes the adjoint. Majorana fermions arise for $d = 2$. This is an example of a planar para algebra, for which the general theory provides diagrammatic representations: for elements of this algebra, and for the representation of its action on Hilbert space.

2.2. **Diagrammatic Representation.** We introduce diagrams to represent elements of our algebra or qudits. The diagrams multiply from bottom to top[2]. Also, tensor products multiply from left to right. We represent the horizontal multiplication XY and the tensor product $X \otimes Y$ by

---

[1]They give this criterion in Theorem 4.1 of [4]. The preprint and published paper are organized differently, and we refer to the numbering in the latter. See also [3].

[2]This follows standard conventions for braids, while the standard convention for circuits is multiplication from left to right.
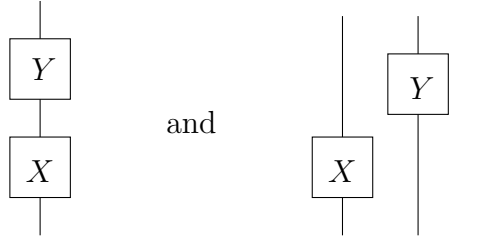
We represent a generator c_j in the jth tensor factor as

$$c_j \text{ replaced by } \Big|\Big| \cdots \Big|1\Big| \cdots \Big|\Big| \; .$$
$$\phantom{c_j \text{ replaced by } \Big|\Big| \cdots \Big|}j$$

The power c_j^α of c_j arises from replacing the label "1" by the label "α."
Additionally,

$$\left.\begin{array}{c}\beta\\ \alpha\end{array}\right| \;=\; \alpha+\beta\Big| \; , \qquad \text{and} \qquad d\Big| = \Big| \; .$$

The parafermion relation (1) becomes

$$\alpha\Big|\Big| \cdots \Big|\begin{array}{c}\beta\\ \,\end{array} = q^{\alpha\beta} \; \begin{array}{c}\alpha\\ \,\end{array}\Big|\Big| \cdots \Big|\beta \qquad \text{for } j < k \; ,$$
$$j \qquad k \qquad\qquad\quad j \qquad k \tag{2}$$

where the strings between j and k contain no excitations. We call $q^{\alpha\beta}$ the twisting scalar. We also remark that the diagrammatic interpretation given in [12] of the twisted tensor product $X \circ Y = \zeta^{|X||Y|} XY$ introduced in [13, 11], interpolates between the left and right side of the parafermion relation (2). We write the labels on the same vertical height. Here ζ is a square root of q, with the property $\zeta^{d^2} = 1$, so

$$\alpha\Big|\Big| \cdots \Big|\begin{array}{c}\beta\\ \,\end{array} = \zeta^{\alpha\beta} \; \begin{array}{c}\alpha\\ \,\end{array}\Big|\Big| \cdots \Big|\beta \qquad \text{for } j < k \; .$$
$$j \qquad k \qquad\qquad\quad j \qquad k \tag{3}$$

The diagram called a *cap* is not an element of the parafermion algebra. Rather it produces qudits. We transport the qudit label from left to right on the cap, producing a phase ζ, which can be interpreted as a Fourier transform relation, see [12]. The cap has the form

$$\alpha \,\frown\; = \zeta^{\alpha^2} \,\frown\, \alpha \;.$$

The related *cup* diagram represents a measurement of the qudit. It also satisfies a Fourier parafermion relation

$$\alpha \smile = \zeta^{-\alpha^2} \smile \alpha \ .$$

We represent the adjoint * diagrammatically as

$$* : \ 1 \ \Big| \ \longrightarrow \ d{-}1 \ \Big| \ . \tag{4}$$

More generally, the adjoint * of a product comes from its vertical reflection,

$$\left(\begin{array}{c} \text{\tiny||||} \\ \boxed{Y} \\ \text{\tiny||} \\ \boxed{X} \end{array} \right)^{*} = \begin{array}{c} \boxed{X^*} \\ \text{\tiny||} \\ \boxed{Y^*} \\ \text{\tiny||||} \end{array} \ .$$

2.3. **Trace.** The normalized trace $\mathrm{tr}(\cdot)$ is represented diagrammatically as

$$\mathrm{tr}\left(\ \Big| \ \Big| \ \right) = \tfrac{1}{\delta} \ \bigcirc = 1,$$

$$\mathrm{tr}\left(\ \mathrm{k} \ \Big| \ \right) = \tfrac{1}{\delta} \ \mathrm{k} \bigcirc = 0 \qquad \text{for } 1 \le k \le d-1 \,.$$

Here $\delta = \sqrt{d}$ represents the circle diagram constant,

$$\delta \ = \ \bigcirc \ .$$

2.4. **Inner Product.** The standard, or computational, basis of the $\mathbb{Z}_d$ graded Hilbert space $\mathcal{H}_d(m)$ is $|i_1 i_2 \cdots i_m\rangle \equiv |i_1\rangle \otimes |i_2\rangle \otimes \cdots \otimes |i_m\rangle$, for $0 \leqslant i_1, i_2, \ldots, i_m \leqslant d-1$. This vector is graded by $\sum_{k=1}^{m} i_k \mod d$. We represent this vector diagrammatically with

$$|i_1 i_2 \cdots i_m\rangle \quad \text{replaced by} \quad \begin{array}{cccc} & & & i_m \\ \Big| & \Big| & \cdots & \Big| \\ i_1 & i_2 & & \end{array} \ . \tag{5}$$

The inner product is represented diagrammatically with

$$\langle x|y \rangle \quad \text{replaced by} \qquad \qquad \qquad \qquad \qquad \qquad \qquad \qquad \tag{6}$$

for $x, y \in \mathcal{H}_d(m)$.

2.5. Partial Trace.
Planar parafermion algebras are half-braided, allowing a partial trace to be defined. The partial trace $\text{tr}^{j_1, j_2, \cdots, j_k}(\cdot)$ for $1 \leq j_1, j_2, \cdots, j_k \leq m$ is represented diagrammatically as

$$\text{tr}^{j_1, j_2, \cdots, j_k}\left(\boxed{X} \right) = \frac{1}{\delta^k} \quad \boxed{X} \quad j_1 \; j_2 \cdots j_k \; .$$

On the right hand side the $j_1, j_2, \cdots, j_k$ strings are closed to form caps. The nonclosed strings are always under the caps. Moreover, the strings were closed clockwise from top to bottom in the illustration. The spherical condition allows strings to be closed counterclockwise from top to bottom. See §2.2 of [12] for details and the definition of the spherical condition.

2.6. Measurement.
A measurement of the $j_1, j_2, \cdots, j_k$ strings is represented diagrammatically as

$$j_1 \mid j_2 \mid \cdots \mid j_k \mid$$

$$\tag{7}$$

To measure we place the meter in (2)

below the $j_1, j_2, \cdots, j_k$ strings,

$$j_1 \mid j_2 \mid \cdots \mid j_k \mid$$

The meter designates that the $j_1, j_2, \cdots, j_k$ strings are to be closed from top to bottom to form caps. We proceed by removing the meter from the diagram and closing the $j_1, j_2, \cdots, j_k$ strings, as discussed above for the partial trace.

In the following example we illustrate a measurement for parafermions of order d. Consider three parafermions in the computational basis

$$i_1 \mid i_2 \mid i_3 \mid$$

Suppose we want to measure the first two tensor factors. We place the meter under the first two strings as illustrated below,
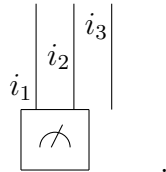
$$i_1 \mid i_2 \mid i_3 \mid$$

The meter under the first two strings designates that those strings are closed to form caps such that

$$\frac{1}{\delta^2} \; i_1 \bigcirc \; i_2 \bigcirc \; i_3 \mid$$

3. Particles

For fermions and parafermions the parafermionic Fock space $\mathcal{H}_d(m)$ is isomorphic to the m-qudit space $\mathbb{C}^{d^m}$, where d denotes the parafermion

order and m is the number of modes. The choice of $d = 2$ is the standard Fock space for m fermionic modes, which is isomorphic to the m-qubit space [17].

The notion of fermionic entanglement for pure states was analyzed in [5], whereby product states are those that one can write as a tensor product in the Fock representation. This definition of entanglement naturally generalizes to the case of parafermionic pure states. We refer to this generalization as *parafermionic entanglement*.

3.1. **The Braid.** Effects of braiding in field theory and quantum Hall systems were considered extensively by Fröhlich, e.g. [9]. Diagrammatic notation in quantum information theory originated in the quantum circuit model of Deutsch [7], although without the consideration of topology. For higher dimensional quantum information in this framework the definition of quantum gates requires several choices. Alternatively, the unitary braid operator in Figure 3 canonically generates maximal fermionic and parafermionic entanglement for arbitrary finite dimensions. See §6.5 of [12] for details and the definition of the braid

$$\diagdown\diagup \equiv \frac{\omega^{-\frac{1}{2}}}{\sqrt{d}} \sum_{k=0}^{d-1} \begin{vmatrix} \mathrm{k} \\ {} \end{vmatrix} \begin{vmatrix} {} \\ -k \end{vmatrix}$$

FIGURE 3. Braid diagram for entanglement.

where $\omega = \frac{1}{\sqrt{d}} \sum_{j=0}^{d-1} \zeta^{j^2}$. We note that the braid has the special property that qudit generators can move under the braid crossing as illustrated in Figure 2.

The braid is unitary, so the adjoint braid equals the inverse braid. Diagrammatically the adjoint is obtained by a vertical reflection, hence the inverse braid is

$$\diagup\diagdown \equiv \frac{\omega^{\frac{1}{2}}}{\sqrt{d}} \sum_{k=0}^{d-1} \begin{vmatrix} {} \\ \mathrm{k} \end{vmatrix} \begin{vmatrix} -k \\ {} \end{vmatrix} . \tag{8}$$

The inverse braid acts by canonically disentangling fermionic and parafermionic states of arbitrary finite dimension.

In the following example we illustrate maximal entanglement for the fermionic case $d = 2$. Consider the two-qubit space

$$\mathbb{C}^4 = \mathrm{Span}_{\mathbb{C}} \left\{ \begin{vmatrix} {} \\ {} \end{vmatrix}, \begin{vmatrix} 1 \\ 1 \end{vmatrix}, \begin{vmatrix} {} \\ 1 \end{vmatrix}, \begin{vmatrix} -1 \\ 1 \end{vmatrix} \right\},$$

in which the braid acts on the basis by

$$\text{(diagram)} = \frac{\omega^{-\frac{1}{2}}}{\sqrt{2}}\left(\Big|\Big|\Big| - {}_1\Big|{}^{-1}\Big|\right) , \tag{9}$$

$$\text{(diagram)} = \frac{\omega^{-\frac{1}{2}}}{\sqrt{2}}\left(\Big|_1\Big| - {}_1\Big|\Big|\right) , \tag{10}$$

$$\text{(diagram)} = \frac{\omega^{-\frac{1}{2}}}{\sqrt{2}}\left(\Big|_1\Big| + {}_1\Big|\Big|\right) , \tag{11}$$

$$\text{(diagram)} = \frac{\omega^{-\frac{1}{2}}}{\sqrt{2}}\left(\Big|\Big| + {}_1\Big|{}^{-1}\Big|\right) . \tag{12}$$

In quantum computation the braid is "imprimitive" in the sense of the Brylinskis, since it is *entangling*. This result yields a partial topological quantum computer for fermions and parafermions. Additionally, the braid may be applied to diagrammatically construct several quantum information protocols, which utilize entanglement as a resource.

4. Qudit X, Y, Z Matrices

One can express the qudit Pauli operators X, Y, Z that satisfy the relations

$$X^d = Y^d = Z^d = 1 , \tag{13}$$

$$YX = q\,XY , \quad ZY = q\,YZ , \quad \text{and} \quad XZ = q\,ZX . \tag{14}$$

Here $q = e^{\frac{2\pi i}{d}}$. These matrices must also satisfy a second set of relations defined in terms of a square root $\zeta = q^{\frac{1}{2}}$ for which $\zeta^{d^2} = 1$, namely

$$XYZ = YZX = ZXY = \zeta^{-1} . \tag{15}$$

In §4 of [12] we give two different solutions $\widehat{X}, \widehat{Y}, \widehat{Z}$ for X, Y, Z in terms of four qudit generators c_1, c_2, c_3, c_4. In §5 of that paper we give a diagrammatic interpretation for these operators. Our first solution has the form

$$\widehat{X} = \zeta\, c_1^{-1}c_4 , \quad \widehat{Y} = \zeta\, c_2 c_4^{-1} , \quad \widehat{Z} = \zeta\, c_3^{-1}c_4 . \tag{16}$$

These matrices satisfy relations (13)–(14), but they do not identically satisfy (15).

As explained in [12], the product $\widehat{X}\widehat{Y}\widehat{Z}$ has the form

$$\widehat{X}\widehat{Y}\widehat{Z} = \widehat{Y}\widehat{Z}\widehat{X} = \widehat{Z}\widehat{X}\widehat{Y} = \zeta^{-1}\gamma \,, \quad \text{where} \quad \gamma = q c_1^{-1} c_2 c_3^{-1} c_4 \,. \quad (17)$$

These relations also show that the unitary grading matrix γ commutes with $\widehat{X}$, $\widehat{Y}$, $\widehat{Z}$. Hence these matrices act on the eigenspaces of γ. One achieves the missing relations (15) by restricting to the subspace for which the grading γ has eigenvalue $+1$. The solution (16) is a generalization of the $d = 2$ map that is common in condensed-matter physics.

Our second solution is

$$\widehat{X} = \zeta \, c_1^{-1} c_2 \,, \quad \widehat{Y} = \zeta \, c_1 c_3^{-1} \,, \quad \widehat{Z} = \zeta \, c_1^{-1} c_4 \,. \quad (18)$$

These matrices $\widehat{X}$, $\widehat{Y}$, $\widehat{Z}$ also satisfy the relations (13)–(15) on the same eigenspace of γ. One can perform this construction at each one of various sites labelled by a subscript j, giving rise to a representation of operators $\widehat{X}_j, \widehat{Y}_j, \widehat{Z}_j$ at each site, and that mutually commute at different sites.

Diagrammatically our two solutions (16) and (18) lead to very different looking models, which in §6 we call four-string models (each string representing a qudit) of Type I and Type II. In the related paper [12], we give details and develop these results in a more general context.

5. Protocols

5.1. **Entanglement distribution.** We apply the braid to construct the entanglement distribution protocol. Consider the computational basis for two parafermions of order d,

$$\left| \begin{matrix} & i_2 \\ i_1 & \end{matrix} \right| \qquad \text{for} \quad 0 \le i_1, i_2 \le d-1.$$

We act with the braid of Figure 3 to generate maximal entanglement, namely

$$i_1 \left| \begin{matrix} i_2 \\ \end{matrix} \right| = \frac{\omega^{-\frac{1}{2}}}{\sqrt{d}} \sum_{k=0}^{d-1} k+i_1 \left| \begin{matrix} \\ -k+i_2 \end{matrix} \right| . \quad (19)$$

The special case of fermions was shown in (9)–(12). The remaining step of the protocol involves distribution of the entanglement through

a noiseless quantum channel [18]. Such a channel leaves (19) invariant. Physically the distribution is performed by a variety of methods [1, 6].
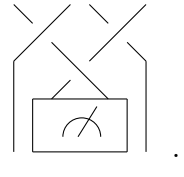
5.2. **Entanglement-swapping.** We can also apply the braid to construct the entanglement-swapping protocol. This protocol inputs four disentangled fermionic or parafermionic states, and maximally entangles two of the states without trivially braiding them. Physically these entangled states do not need to share any common past [20].

Consider the diagram below, which entangles the first and second strings, and it entangles the third and fourth strings. Then, it disentangles the second and third strings with the inverse braid:

$$\tag{20}$$
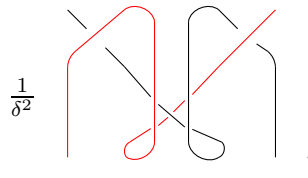
We proceed by placing the meter, introduced in §2.6, under the second and third strings of (20), as illustrated below

$$\tag{21}$$

We claim that (21) acts by maximally entangling the leftmost and rightmost input states as desired. Here we use the relations in §6.5 of [12].

We remove the meter in (21), closing the second and third strings to form caps as illustrated below

$$\frac{1}{\delta^2} \tag{22}$$

Isotopy is a property of parafermion planar algebra. This topological notion simplifies the computation of (22) and reduces it to a scalar multiple of the braid. It permits us to move the strings in three-dimensional space. We note that the red string under the Reidemeister moves becomes the braid's over crossing. We use the second Reidemeister move on (22) to obtain

$$\frac{1}{\delta^2} \qquad \qquad . \tag{23}$$

Application of the second and third Reidemeister moves simplifies the diagram above to

$$\frac{1}{\delta^2} \qquad \qquad . \tag{24}$$

The braid and its inverse in (24) have opposite coefficients by the first Reidemeister move, reducing the diagram to

$$\frac{1}{\delta^2} \qquad \qquad . \tag{25}$$

Therefore, the entanglement-swapping diagram in (21) maximally entangles the leftmost and rightmost input states without trivially braiding them. We note that in contrast to the topological moves used that the algebraic approach of expanding the braid into a sum of the basis leads to a complicated computation for (22).

The entanglement-swapping protocol with braids holds for arbitrary finite dimensions. In Figure 4 we illustrate the fermionic case $d = 2$.
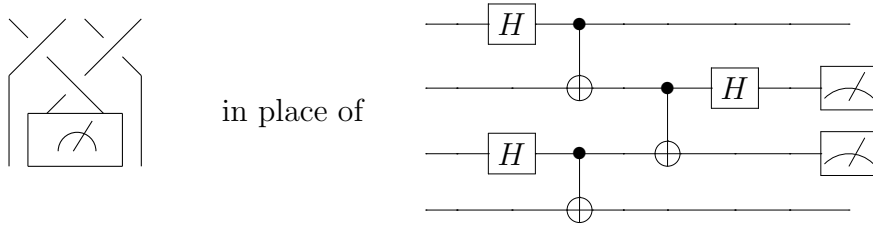
FIGURE 4. Entanglement-swapping with braids on the left, and a quantum circuit on the right.

Remark: Pictorial representation of other protocols, such as teleportation, superdense coding, and the EPR protocol for quantum key distribution, could be studied by these methods.

6. Different models for quantum information

We contrast one-string, two-string, and four-string models, in order to represent quantum information in terms of diagrams. The qudits are given by Majoranas, parafermions, or bosons, respectively.

6.1. **The One-String Model.** In the bulk of this paper, we realized a qudit by one labeled string. Transformations on m qudits were realized by diagrams with m input points and m output points. We call this representation of quantum information the *one-string model*. In this model the Hilbert space is $\mathbb{Z}_d$ graded. So, the transformations act on different components as the graded tensor product. We note that the diagrams used in the previous sections, such as the braid, are zero graded, or globally gauge invariant. Thus, the twisting scalar $q^{\alpha\beta} = 1$, which reduces the graded tensor product to the usual tensor product.
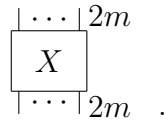
6.2. **The Type I, Two-String Model.** For the two-string models, each qudit is a parafermion. In the *type I, two-string model*, we realize a qudit by one labeled cap

$$k \overset{\frown}{} .$$
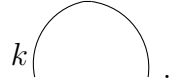
Here $0 \leq k \leq d - 1$. We represent m-qudits by
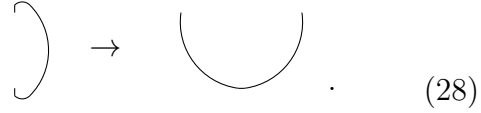
$$k_1 \overset{\frown}{} \quad k_2 \overset{\frown}{} \quad \cdots \quad k_m \overset{\frown}{} \quad .$$

A transformation on m-qudits is represented by

$$\boxed{X}\, \genfrac{}{}{0pt}{}{|\cdots|\,2m}{|\cdots|\,2m} \quad .$$

The one-string model can be embedded into the type I two-string model by making the following replacements:

$$\text{Qudit}: \qquad k\,\Big| \quad \rightarrow \quad k\overset{\frown}{} \, , \tag{26}$$

$$\text{Transformation}: \qquad \boxed{X}\,\genfrac{}{}{0pt}{}{|\cdots|}{|\cdots|} \quad \rightarrow \quad \boxed{X} \, , \tag{27}$$

$$\text{Measurement}: \qquad \Big) \quad \rightarrow \quad \bigcup \bigcup \quad . \tag{28}$$
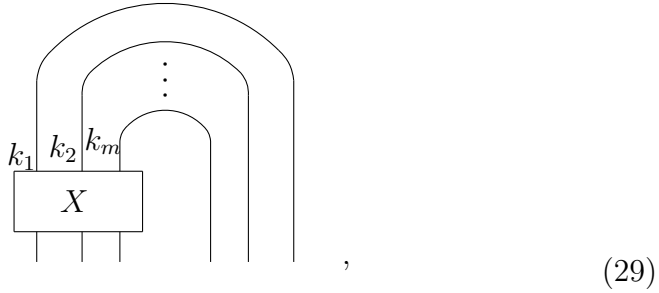
6.3. **The Type II, Two-String Model.** In the type II, two-string model, we represent m-qudits by labeled caps

$$k_1 \quad k_2 \quad k_m \qquad .$$
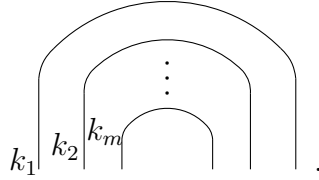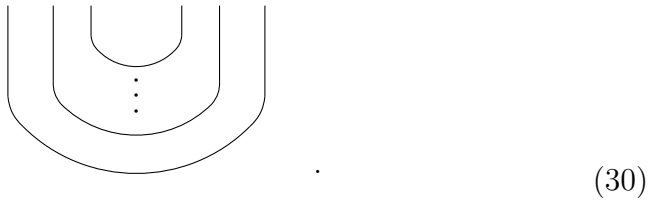
A transformation on m-qudits is represented by

$$\boxed{X} \begin{array}{c} | \cdots | 2m \\ \\ | \cdots | 2m \end{array} \quad .$$
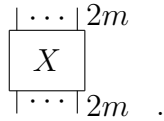
The one-string model can be embedded into the type II two-string model by replacements of a transformation similar to (27), and by using

$$k_1 \quad k_2 \quad k_m \quad \boxed{X} \qquad , \tag{29}$$

and the measurement

$$\qquad \qquad . \tag{30}$$

6.4. **The Four-String Model.** For the four-string model, each qudit is bosonic. In other words a qudit always has particle-antiparticle pairs that yield a total grading zero. For the type I four-string model, we

realize a qudit by two labeled caps. We represent m-qudits by the picture:
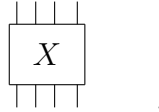

Here $0 \leq k_i \leq d - 1$.

For the type II four-string model, we represent m-qudits by the diagram:
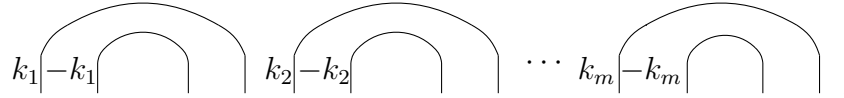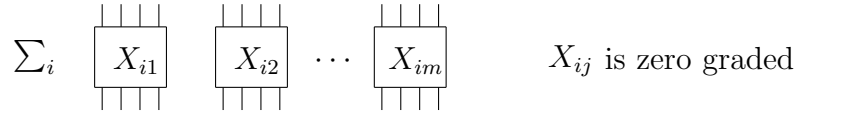

Again $0 \leq k_i \leq d - 1$.

A transformation on a single qudit is a zero graded diagram represented by

A transformation on m-qudits is a linear sum of tensor products of m single qudit transformations represented by

$$\sum_i \quad \boxed{X_{i1}} \quad \boxed{X_{i2}} \quad \cdots \quad \boxed{X_{im}} \qquad X_{ij} \text{ is zero graded}$$

We note that the four-string model is different from the one-string model and the two-string model, where all diagrams with proper inputs and outputs are transformations on qudits. In the four-string model we are interested in diagrams that preserve the subspace spanned by qudits, diagrams given by caps. Consider the following diagrammatic example, which is not a transformation on 2-qudits

Let us construct some controlled transformations for the type I four-string model. We define the controlled transformation C_A on 2-qudits as $C_A|ij\rangle = |iA^i(j)\rangle$. On a single qudit, matrices X, Y, Z are constructed as in (16).

We show that the following double braid S preserves 2-qudits, and $S = C_Z^2$.
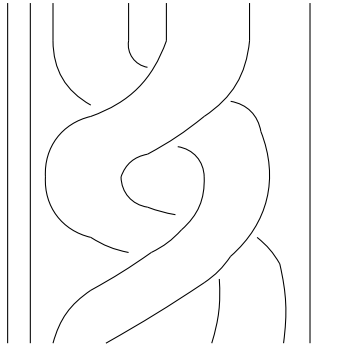
The proof follows from the qudit-braid relation given in Figure 2:

$$= q^{ij}$$

$$= q^{ij}$$

$$= q^{2ij}$$

Let b_i be the braid on the ith and $i+1$th strings

$$b_i = \underset{i \quad i+1}{\Big\diagup} .$$

One can obtain qudit matrices X, Y from Z by the conjugation of braids,

$$Y = b_2^* Z^* b_2;$$
$$X = b_1^* b_2^* Z b_2 b_1.$$

see §5 in [12] for a diagrammatic proof. Thus

$$C_Y^2 = b_6^* S^* b_6;$$
$$C_X^2 = b_5^* b_6^* S b_6 b_5.$$

Therefore, both C_Y^2 and C_X^2 preserve the subspace spanned by qudits and both are presented by braided diagrams.

Acknowledgement

References

[1] M. Asperlmeyer, H. R. Böhm, T. Gyatso, T. Jennewein, R. Kaltenbaek, M. Lindenthal, G. Molina-Terriza, A. Poppe, K. Resch, M. Taraba, R. Ursin, P. Walther, and A. Zeilinger, Long-distance free-space distribution of quantum entanglement, *Science* **01**, Vol. 301 Issue 5633, (2003) 621–623, doi:10.1126/science.1085593.

[2] M. F. Atiyah, Topological quantum field theory, Publications Mathématiques de l'IHÉS **68** (1988), 175–186, doi:10.1007/BF02698547.

[3] M. J. Bremner, C. M. Dawson, J. L. Dodd, A. Gilchrist, A. W. Harrow, D. Mortimer, M. A. Nielson, and T. J. Osborne, Practical scheme for quantum computation with any two-qubit entangling gate, *Phys. Rev. A* **89**, (2002) 247902, doi:10.1103/PhysRevLett.89.247902.

[4] J. L. Brylinski and R. Brylinski, Universal quantum gates, in Mathematics of Quantum Computation, G. Chen and R. K. Brylinski, Editors, Chapman & Hall/CRC, Boca Raton, Florida 2002. http://arxiv.org/pdf/quant-ph/0108062v1.pdf.

[5] M. Bañuls, J. I. Cirac, and M. M. Wolf, Entanglement in fermionic systems, *Phys. Rev. A* **76**, (2007) 022311, doi:10.1103/PhysRevA.76.022311.

[6] J. I. Cirac, H. J. Kimble, and H. Mabuchi, Quantum state transfer and entanglement distribution among distant nodes in a quantum network, *Phys. Rev. Lett.* **78** (1997), 3221, doi:10.1103/PhysRevLett.78.3221.

[7] D. Deutsch, Quantum computational networks, *Proceedings of the Royal Society of London. Series A, Mathematical and Physical Sciences*, Vol. 425, No. 1868 (1989), 73–90, doi:10.1098/rspa.1989.0099.

[8] M. H. Freedman, A. Kitaev, M. J. Larsen, and Z. Wang, Topological quantum computation, *Bulletin of the American Mathematical Society* Volume 40, Number 1, (2002), 31–38, doi:10.1090/S0273-0979-02-00964-3.

[9] J. Fröhlich, New super-selection sectors ("Soliton-States") in two-dimensional Bose quantum field models, *Commun. Math. Phys.* **47** (1976), 269–310.

[10] A. Hutter and D. Loss, Quantum computing with parafermions, (2015), http://arxiv.org/pdf/1511.02704v1.pdf.

[11] A. M. Jaffe and B. Janssens, Characterization of reflection positivity, *Commun. Math. Phys.*, to appear. http://arxiv.org/abs/1506.04197

[12] A. M. Jaffe and Z. Liu, Planar para algebras, reflection positivity, to appear.

[13] A. M. Jaffe and F. L. Pedrocchi, Reflection positivity for parafermions, *Commun. Math. Phys.*, **337** (2015), 455–472.

[14] V. F. R. Jones, Hecke algebra representations of braid groups and link polynomials, *Ann. of Math* **126** (1987), no. 2, 335–388, doi:10.2307/1971403.

[15] L. Kauffman and S. Lomonaco Jr., Braiding operators are universal quantum gates, *New J. Phys.* **6** (2004) 134, doi:10.1088/1367-2630/6/1/134.

[16] A. Kitaev, Fault-tolerant quantum computation by anyons, arXiv:quant-ph/9707021, *Annals of Physics* Volume 303, Issue 1, (2003) 2–30, doi:10.1016/S0003-4916(02)00018-0.

[17] M. A. Nielsen, The Fermionic canonical commutation relations and the Jordan-Wigner transform, (2005).

[18] M. M. Wilde, Quantum Information Theory, *Cambridge University Press* 2013, 136–176.

[19] E. Witten, Topological quantum field theory, *Comm. Math. Phys.* **117** (1988), no. 3, 353–386, http://projecteuclid.org/euclid.cmp/1104161738.

[20] M. Zukowski, A. Zeiling, M. A. Horne, and A. K. Ekert, "Event-ready-detectors" Bell experiment via entanglement swapping, *Phys. Rev. Lett.* **71**, (1993) 4287, doi:10.1103/PhysRevLett.71.4287.